

Article



# The directivity of noise radiated by a railway wheel in situ

Proc IMechE Part F: J Rail and Rapid Transit 2025, Vol. 0(0) 1–10 © IMechE 2025



Article reuse guidelines: sagepub.com/journals-permissions DOI: 10.1177/09544097251343733 journals.sagepub.com/home/pif



Xianying Zhang<sup>1,2,3</sup>, Yuan He<sup>4</sup>, David J. Thompson<sup>3</sup> and Zhiwei Hu<sup>4</sup>

#### **Abstract**

The most important noise source from railways is rolling noise, which is produced by vibration of the track and wheel, induced by their combined surface roughness. The component of noise radiated by the wheel is generally the greatest above 2 kHz and increases in overall importance as the train speed increases. The current models used to predict the sound radiation from the wheel consider this to be located in free space; in practice, however, the rail beneath the wheel, the ground in close proximity, the presence of the bogie frame around it and the train body above it can modify the wheel radiation. This paper investigates the influence of these factors on the sound power and the directivity of the wheel in both vertical and horizontal planes. The sound radiation of the wheel is analysed by using a combination of the Finite Element Method for vibration and the acoustic Boundary Element Method with Adaptive Order in three dimensions. The geometries of the rail, ground, bogie frame and the train body are introduced in the acoustic model to investigate their influence on the sound radiation from the wheel. It is shown that these nearby structures affect the sound power of the wheel only at low frequency, but they have a significant influence on the directivity of the sound in the whole frequency range. Of the various structures considered, the presence of the rail and the bogie frame has little effect on the wheel radiation, whereas the ground and car body have a greater effect. Finally, new approximate expressions are developed for the wheel directivity in the presence of the train body that can be used in engineering models.

#### **Keywords**

Railway wheel, sound radiation, superstructure, railway rolling noise prediction, railway vehicle

Date received: I March 2025; accepted: 5 May 2025

#### Introduction

For trains running at conventional speeds, or even for high-speed trains with speeds up to 350 km/h, rolling noise is the most important noise source in the railway system. It is generated by the vibration of the track and wheel induced by their combined surface roughness at the wheel/rail contact area. The component radiated by the wheel dominates the noise above 2 kHz and its relative importance, in terms of the overall level, increases with increasing train speed. It is therefore important to understand the properties of the wheel vibration and sound radiation before implementing cost-effective noise reduction measures in the railway system.

In prediction models for rolling noise, the sound radiation from the wheel is commonly calculated assuming it to be located in free space due to the computational expense of models including more features. Early models treated the wheel noise as the superposition of a series of simple point sources. Models were developed in Refs. 3 and 4 based on a Rayleigh integral formulation. Fingberg later adopted the boundary element method (BEM) to predict the sound radiation from wheels, susing an axisymmetric formulation in which the wheel was represented only by its cross-section. It was shown that the radiation ratio differed significantly at low frequencies from that predicted by the Rayleigh integral method, whereas differences of less than

2 dB were found at high frequencies. In Ref. 6, the combination of the finite element method (FEM) and acoustic BEM have been used to calculate the wheel radiation, leading to a series of parametric formulae that were proposed to predict the sound radiation efficiency of the wheel with different axial and radial motions. These have been implemented in the TWINS model for rolling noise. The wheel directivity is approximated as a monopole for radial motion or as a dipole for axial motion. The combination of the combination of the finite element method (FEM) and acoustic BEM have been used to calculate the wheel radiation, leading to a series of parametric formulae that were proposed to predict the sound radiation efficiency of the wheel with different axial and radial motion.

Cheng et al. investigated the influence of various common assumptions in modelling the vibration of a wheelset on its radiated sound power by using a combined FEM and BEM approach.<sup>9</sup> It was shown that neglecting the

### Corresponding author:

David J. Thompson, Institute of Sound and Vibration Research, University of Southampton, Highfield, Southampton, SO17 IBJ, UK.

Email: djt@isvr.soton.ac.uk

<sup>&</sup>lt;sup>1</sup>Key Laboratory of Road and Traffic Engineering of the Ministry of Education, Tongii University, Shanghai, China

<sup>&</sup>lt;sup>2</sup>Shanghai Key Laboratory of Rail Infrastructure Durability and System Safety, Tongji University, Shanghai, China

<sup>&</sup>lt;sup>3</sup>Institute of Sound and Vibration Research, University of Southampton, Southampton, UK

<sup>&</sup>lt;sup>4</sup>Aerodynamics and Flight Mechanics Group, Faculty of Engineering and Physical Sciences, University of Southampton, Southampton, UK

wheel rotation could lead to differences of up to 3 dB. The influence of wheel rotation on the vibration and sound power of a wheelset was also studied by Knuth et al. in a rolling noise prediction model for a wide range of speeds. <sup>10</sup> It was shown that representing the wheel rotation with a moving load approach, i.e. neglecting inertial effects, <sup>11</sup> provides a suitable approximation for use in rolling noise predictions.

The effect of source motion was studied by Sheng et al. by establishing the boundary integral equations. <sup>12</sup> They considered the sound radiation of a harmonically vibrating body with uniform motion in a free field and applied this to a pulsating sphere. They showed that the source motion leads to the well-known Doppler frequency shift and convective amplification. Both the rotational and translational motion of the wheelset were considered by Sheng et al. in predicting the rolling noise of wheels running at high-speed on slab tracks. <sup>13</sup> The wheel sound power was determined using BEM but the sound pressure during the pass-by was calculated using an equivalent monopole.

A computationally efficient approach was recently proposed by Theyssen et al. for calculating the pass-by sound pressure from railway wheels in the time domain using moving Green's functions. <sup>14</sup> A modal approach was introduced in which the pass-by sound radiated by each wheel mode is calculated separately. To improve the calculation efficiency, equivalent sources were then introduced based on spherical harmonics.

In all the studies introduced above, the wheel is assumed to be radiating into free space. The effect of the presence of the ground and the surrounding structures, such as the train body, on the wheel radiation has also been studied by some authors. Experimental work was conducted by Zhang and Jonasson<sup>15</sup> to investigate the directivity of the wheel radiation in different situations. This included measurements in a free field and in the presence of a track and ground, as well as with the inclusion of a simplified train body mockup. Fabre et al. 16 found that a rigid ground had no influence on the radiation ratio of a wheel above 150 Hz, but it had some effect on its sound pressure. Field measurements conducted by Heng showed that the rolling noise during a train passage had a vertical directivity pattern with the maximum sound pressure level at about 60° to the horizontal; at larger angles the sound was shielded by the vehicle body. 17 However, the geometrical influence of the different structures in close proximity to the wheel on its sound radiation remains unclear and warrants further investigation.

The aim of this paper is to carry out a systematic study into the effects of surrounding structures on the sound power and directivity of the wheel, to approximate more closely the geometrical conditions of a wheel in situ within a train. This builds on a preliminary numerical study by the authors. <sup>18</sup> For the purpose of this comparative study, the effect of wheel rotation and motion is neglected. The vibration of the wheel is first calculated using a Finite Element model. This is used as input to calculations of the wheel sound radiation under different boundary conditions. These use the Boundary Element Method with Adaptive Order (BEMAO), which is implemented in the software Simcenter 3D, <sup>19–21</sup> and has the advantage of greatly improved

computational efficiency.<sup>22</sup> The method is verified by comparisons with measured results of the directivity from the literature. The directivity of the wheel in the presence of various nearby structures is then investigated numerically, and finally new simplified formulae are proposed for the wheel directivity in the presence of the train body, that can be used in engineering models.

#### Models for wheel radiation

# Numerical models for wheel vibration

The wheel studied in this paper is a typical straight-web wheel with a diameter of 0.92 m, from a Chinese high-speed train. The sound radiation from this railway wheel is numerically calculated by a combination of the finite element method and the boundary element method. Its vibration is first predicted in the Simcenter 3D software using the finite element method. The model is shown in Figure 1; the material properties are those of steel (Young's modulus  $2.1 \times 10^{11}$  Pa, density 7850 kg/m<sup>3</sup>, Poisson's ratio 0.3). Quadratic solid elements are used, with a maximum element size of 45 mm. The mesh is divided into 60 segments in the circumferential direction, which is sufficient to resolve modes with up to 10 nodal diameters.

The wheel noise is dominated by flexible modes with two or more nodal diameters, which are not influenced by the axle. Similar to previous studies, e.g., Refs. 6–8, 14, and 16, the axle is therefore omitted from the model. To consider its influence in a simplified way, and to ensure the correct rigid-body behaviour, the region inside the hub is filled with a material with an elastic modulus and density that are much larger than those of other parts in the wheel. This increased density (53,953 kg/m<sup>3</sup>) is chosen to ensure that the total mass of the wheel model is equivalent to that of half a wheelset. The damping ratio is set to 0.005, which is greater than would apply for a free wheel but is chosen to be more representative of the damping of a wheel in contact with the rail. A unit harmonic force is applied in the vertical and lateral directions at the nominal wheel-rail contact point. The wheel response is calculated at all nodes of the FE model over the frequency range between 20 and 6000 Hz with a step of 10 Hz by using the modal superposition method.

# Numerical models for wheel radiation

The wheel sound radiation is next predicted by using a three-dimensional boundary element model. The wheel vibration obtained from the FE model is extracted on the surface of the structural mesh and applied as the velocity boundary conditions in the acoustic model of the wheel.

To demonstrate the computational efficiency, the calculation times required for the sound radiation from the railway wheel in free space have been compared between the conventional Boundary Element Method (BEM), Fast Multipole Boundary Element Method (FMBEM) and BEMAO. All the computations were run in the Simcenter 3D software on a Windows workstation with Intel® Xeon® Platinum 8383C CPU @2.70 GHz and 1024 GB RAM using the same mesh. The corresponding computational

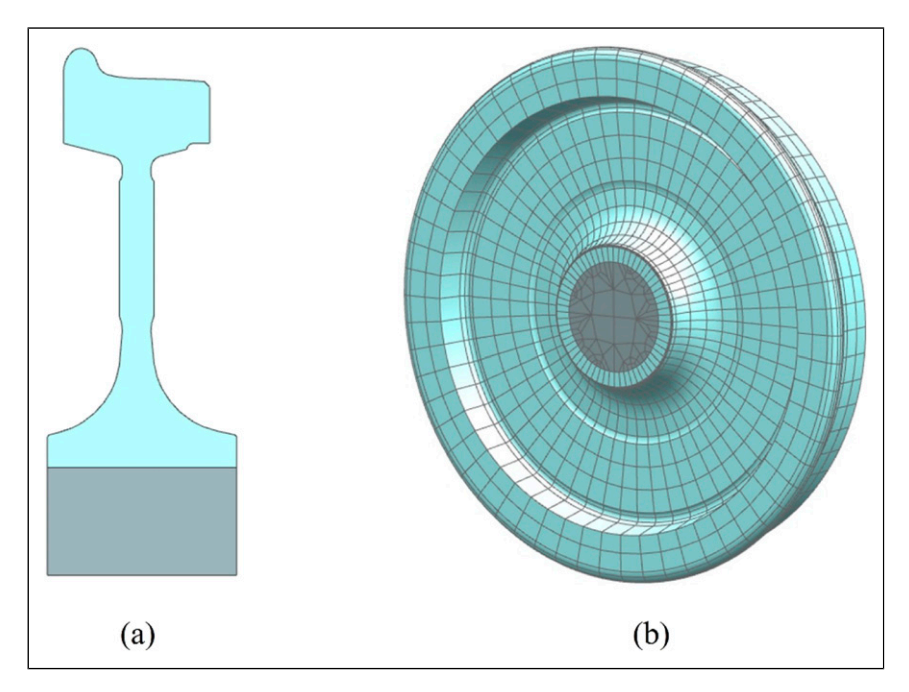


Figure 1. Finite element model of the wheel. (a) Cross-section of the wheel; (b) wheel mesh.

times were: 60 h 21 min for conventional BEM, 18 h 26 min for FMBEM and 1 h 40 min for BEMAO. The calculation results obtained by these three methods (not shown here) were almost identical. More details on the calculation results from the three methods are given in Ref. 22.

## Comparison with measurements

To verify this approach further, comparisons are made with measurements of wheel directivity presented in Refs. 1 and 6. These were for four example vibration modes of the wheel: two axial modes and two radial modes, with natural frequencies between 2.4 and 4 kHz. Although the wheel type was different from the present case, it had a similar diameter and also had a straight web. Comparisons are therefore made with the results calculated at the natural frequencies of the corresponding wheel modes. Field points are selected on a circle at a radius of 1.5 m from the wheel centre with angular positions between 0 and 155° to correspond to those used in Ref. 6. The sound pressure distribution is compared in Figure 2 for these four modes. Although there are some differences between them, for example in the location of minima, reasonable qualitative agreement can be seen. In particular, for the axial modes the radiation is stronger in the lateral direction, whereas for the radial modes it is almost equally strong in the vertical direction.

# Influence of close structures on wheel radiation

# Geometrical models

Five different situations are considered to study the effect of structures in close proximity to the wheel: (i) the wheel is located in free space (reference situation); (ii) it is located 200 mm above a rigid ground plane; (iii) it is located

directly above a rail as well as above the ground; (iv) the bogie frame is additionally located in front of the wheel; (v) and finally the train body is installed above the wheel and bogie frame. The rail in models (iii)-(v) has a length of 5.69 m and is assumed not to vibrate; it is only present to study its scattering effect on the wheel noise. There is a gap in the model of 1 mm between the bottom of the wheel and the top of the rail. Only a single wheel and rail are included in the model as it is those nearest the receiver that are of most importance.

To represent the train body in model (v), a half-length carriage of a Chinese high-speed train is introduced in the model, as shown in Figure 3(a). However, since the acoustic wavelength is much shorter at high frequencies than that at low frequency, the model would become unreasonably large at high frequencies. Consequently, the length and the height of the train vehicle are progressively reduced, giving four different train body models that are adopted in the calculations for different frequency ranges, as illustrated in Figure 3. In each case an overlapping frequency region, spanning a single one-third octave band, is included to ensure continuity. Within these regions, a linear interpolation is carried out between the results of the two models. Finally, the results are converted to one-third octave bands.

### Influence on sound radiation

The sound power radiated by the wheel under these different boundary conditions is shown in one-third octave bands in Figure 4. Results are shown for a unit force excitation at the wheel/rail contact point in both the vertical and lateral directions. The sound power is calculated by integrating the far-field squared pressure over a sphere (for the wheel in free space) or a hemisphere (when the ground is included) at a distance of 15 m away from the wheel. For the radial excitation, in Figure 4(a), high sound power levels are

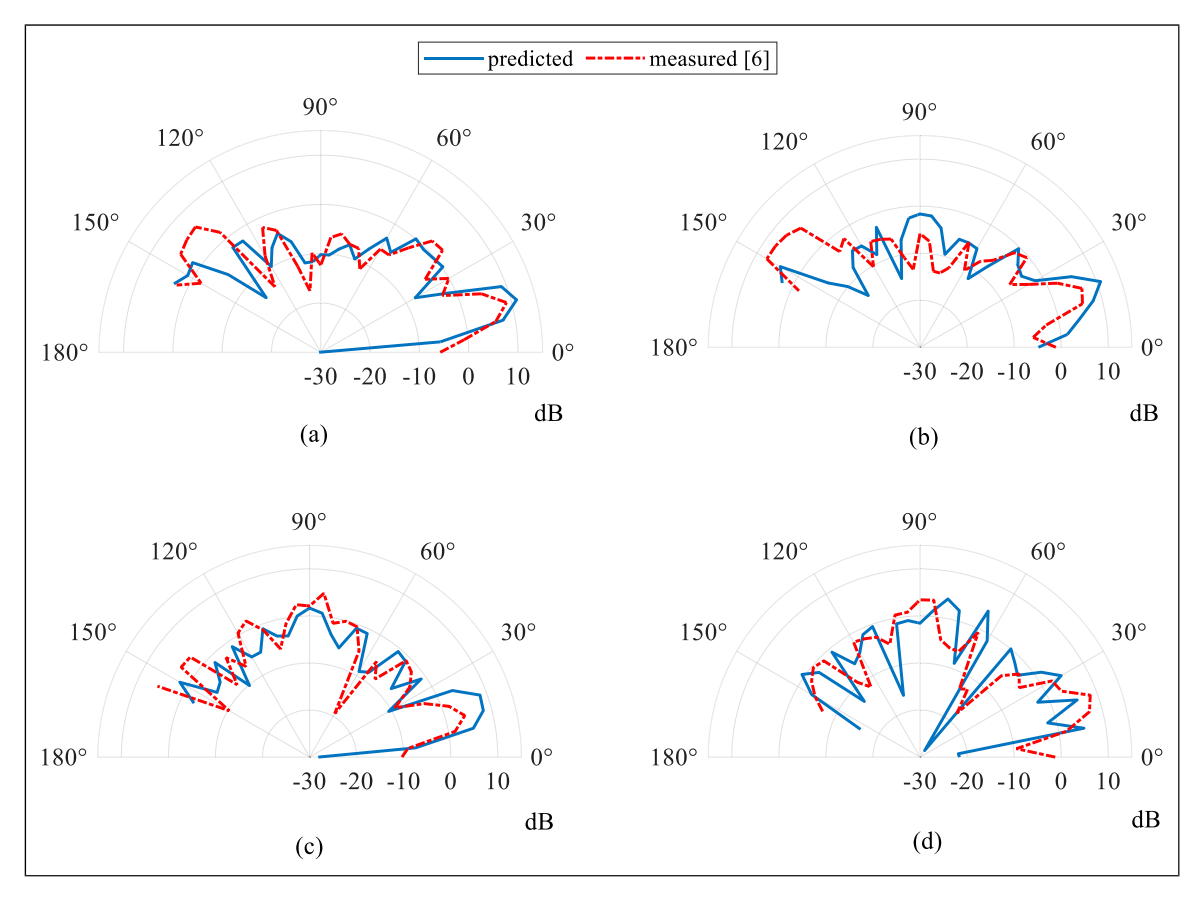


Figure 2. Comparison of the directivity for the wheel in free space between the prediction and the measured data from Ref. 6 (a) 3-nodal-diameter and 1-nodal-circle axial mode; (b) 5-nodal-diameter and 1-nodal-circle axial mode; (c) 3-nodal-diameter radial mode; (d) 5-nodal-diameter radial mode.

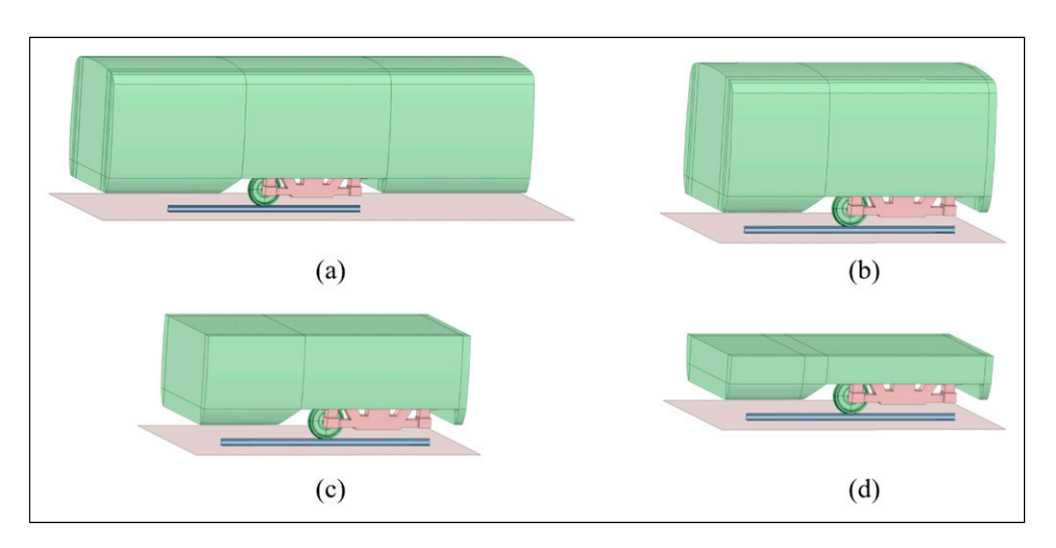


Figure 3. BE models used to include the train body for different frequency regions. (a) Length 12.5 m, height 3.5 m, 20–570 Hz; (b) Length 7.15 m, height 3.5 m, 440–1800 Hz; (c) Length 7.15 m, height 2.35 m, 1400–2820 Hz; (d) Length 7.15 m, height 1.18 m, 2240–5630 Hz.

found at and above 2 kHz due to the radial and one-nodal-circle axial vibration modes of the wheel. 1

In general, the sound power of a source is influenced by its proximity to solid surfaces when they are located within about half the acoustic wavelength.<sup>23</sup> At low frequencies the presence of the ground leads to a slight increase in the sound power from the wheel in Figure 4(a) between 80 Hz and 250 Hz. Apart from this, introducing the rail and bogie frame has little influence on the sound power, whereas the

presence of the train body has a more obvious effect below 160 Hz, where the distance of the train body above the ground is less than half the acoustic wavelength. For the lateral excitation, in Figure 4(b), the rigid ground increases the wheel sound power by around 2 dB below 250 Hz compared with the free wheel; the presence of the rail, bogie frame and train body also affects the wheel sound power in this frequency region. Of these structures, the rail has the most effect.

The sound pressure at the standard measurement point, which is located 7.5 m away from the track centre (6.79 m from the centre of the wheel) and 1.2 m above the top of the rail, is presented in Figure 5. For both excitation directions, the sound pressure level is lower for the wheel in free space than in all other cases. The introduction of the rigid ground increases the sound pressure level at all frequencies except around 1600 Hz. The inclusion of the rail has a negligible effect apart from the additional increase already seen in Figure 4(b) below 250 Hz for lateral excitation. The bogie frame and train body affect the sound pressure to some extent over the whole frequency range, with the train body having most effect at low and mid frequencies.

# Directivity in vertical plane

The directivity of the wheel in a vertical plane is calculated by determining the sound pressure at field points located on a quarter circle, with a radius of 6.79 m, which has its centre at the wheel centre. An angular spacing of  $5^{\circ}$  is used; the

first position, at  $0^{\circ}$ , corresponds to the axis of the wheel, whereas the last position at  $90^{\circ}$  is 6.79 m above the wheel axis.

The results under the different boundary conditions are calculated in each one-third octave band for vertical and lateral excitation. Some results in different frequency bands are shown later. To summarise these results here, Figure 6 presents the directivity in terms of the total sound pressure level for a unit force averaged over all one-third octave bands from 50 to 5000 Hz. For the vertical excitation, these results are mainly dominated by the frequency bands between 2000 Hz and 5000 Hz, as seen from Figure 5(a). For this direction of excitation, the various geometrical structures have little influence on the overall sound directivity of the wheel, which is not strongly directional. The main exception is that the train body reduces the sound radiation considerably between 75° and 90° and increases it slightly elsewhere. The presence of the rigid ground leads to an increase in the sound pressure and the suppression of the onaxis zero found for the case in free space.

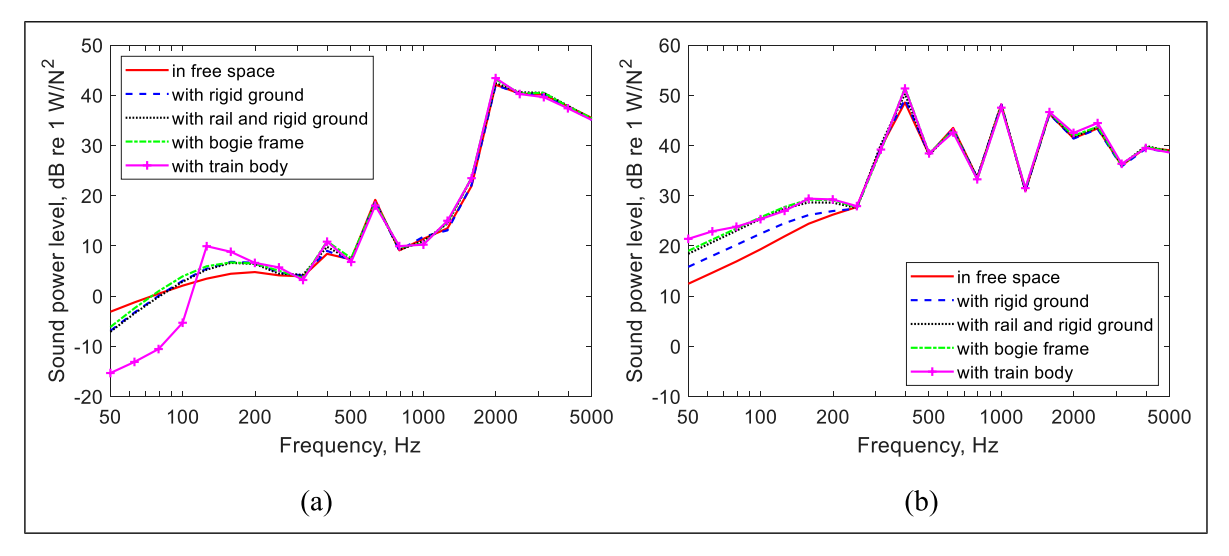


**Figure 4.** Comparison of the sound power level for a unit force under different boundary conditions in one-third octave bands. (a) Vertical excitation; (b) Lateral excitation.

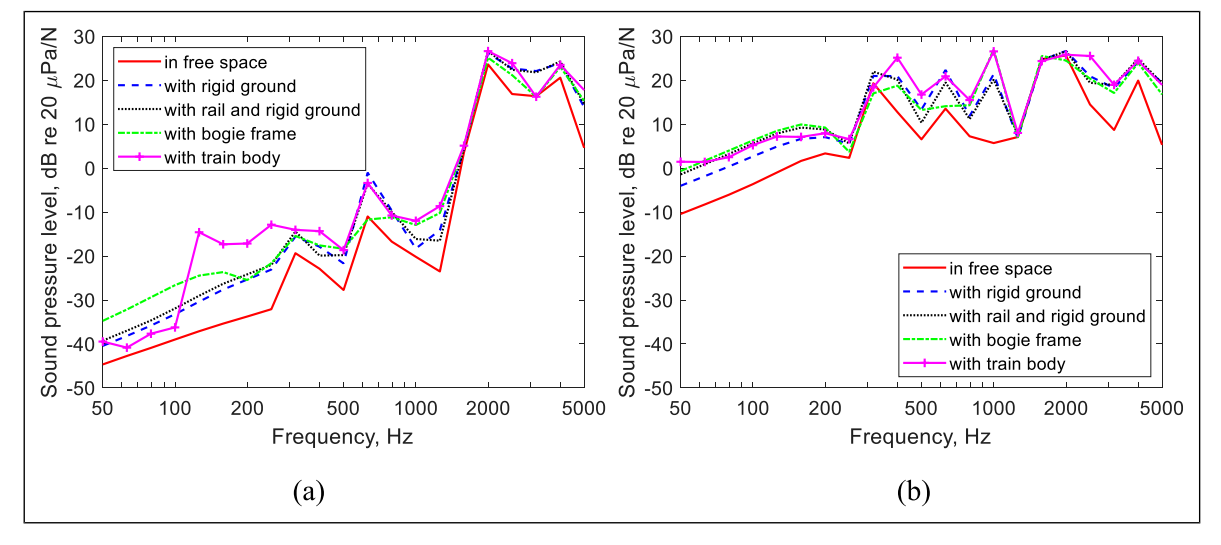


Figure 5. Comparison of the sound pressure level at standard measurement point under different boundary conditions in one-third octave bands. (a) Vertical unit force; (b) Lateral unit force.

For the lateral excitation, the results are dominated by many frequency bands between 400 Hz and 5000 Hz, see Figure 5(b). The wheel radiates in free space approximately like a lateral dipole at low frequencies, with a more complicated pattern at high frequency. The average over the frequency range is shown in Figure 6(b), which retains a pattern like a lateral dipole, with a minimum in the vertical direction.

# Directivity in horizontal plane

To study the variation in the longitudinal direction, the sound pressure level is predicted along a horizontal line at a distance of 7.5 m from the track centreline and 1.2 m above the top of the rail, for distances between -7.5 m and 7.5 m from the wheel axis in the direction parallel to the track. Only the results for the wheel in free space and the full model with the train body are compared here. The results are presented in Figure 7 for vertical and lateral excitation as the average over all one-third octave bands (50–4000 Hz). The presence of the car body changes this directivity to some extent but there is not a strong shielding effect.

Although source motion has been neglected, it is known that it will lead to the Doppler frequency shift and convective amplification<sup>12</sup>; the latter effect is likely to modify the horizontal directivity to some extent for high-speed trains. Wheel rotation has also been neglected. Its main effect is to split the resonance frequencies into pairs, which has some effect on the sound power as well as the frequency spectrum.<sup>10</sup> However, this is unlikely to affect the vertical or horizontal directivities.

# Empirical formulae for the directivity in the presence of the train body

# Directivity in vertical plane

It was shown in Figure 4 that the wheel sound power changes little when various geometrical boundary conditions are applied, so that it can be approximated by the

sound power of the wheel in free space. However, the sound pressure is more obviously affected, especially in the presence of the train body. In this section, expressions are proposed for the wheel directivity to represent the case including the effect of the train vehicle.

For a source radiating sound in an infinite half-space, the relationship between the mean-square pressure and the sound power can be written as

$$\overline{p^2} = \frac{\rho_0 c_0 W}{2\pi r^2} D(\theta) \tag{1}$$

where W is the source sound power,  $D(\theta)$  is the directivity factor,  $\rho_0$  and  $c_0$  are the density of air and the speed of sound, and r is the distance between the sound source and the receiver.

It is assumed that the wheel directivity factor can be approximated by a combination of a monopole source and a dipole source, which can be written as

$$D(\theta) = a + b \cdot 3\cos^2\theta \tag{2}$$

where a and b are constant values, which are the weighting factors for the monopole and dipole sources. For consistency, these must satisfy  $0 \le a \le 1$ ,  $0 \le b \le 1$  and a + b = 1. A curve fitting procedure is used to match the calculations obtained from the BEM predictions of the wheel radiation to the formulae in equations (1) and (2) for each one-third octave band, by minimising the mean square error.

A comparison between the different simple models of directivity and the calculated sound radiation of the wheel in the presence of the train body is shown in example one-third octave bands in Figure 8 for vertical excitation. Similar results (not shown) are found for lateral excitation. The proposed model has a better agreement with the prediction of the wheel radiation over the whole frequency range compared with a pure monopole or dipole source, but the directivity is obviously different from that of the wheel in free space, especially at 0° and 90°. The wheel directivity corresponds to a dipole source at high frequency where it is the dominant noise source in the rolling noise.

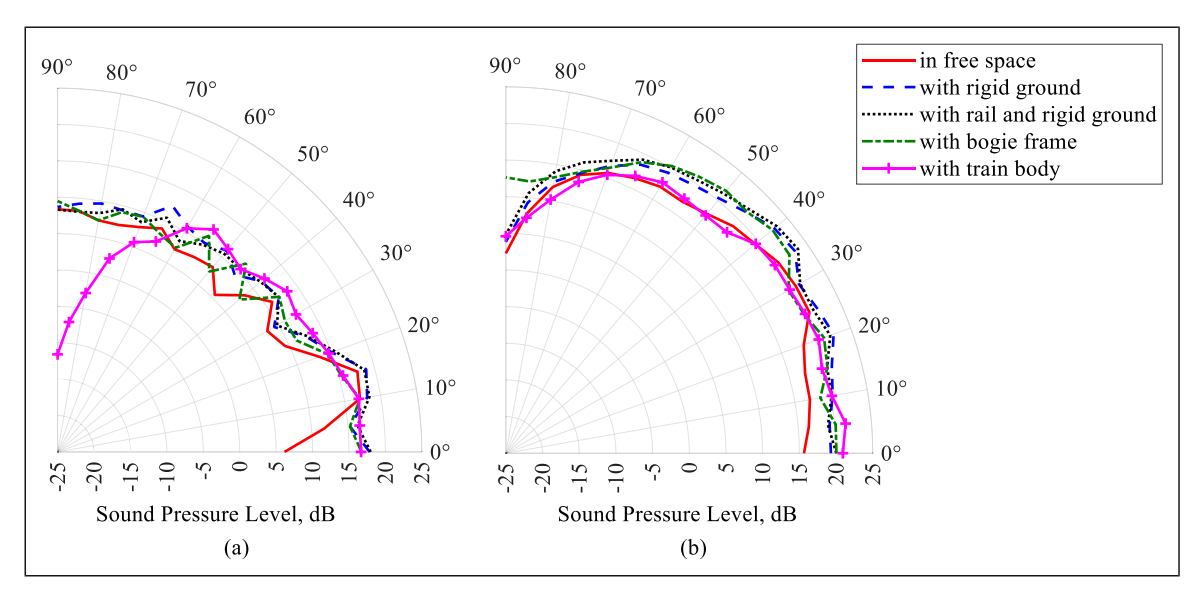
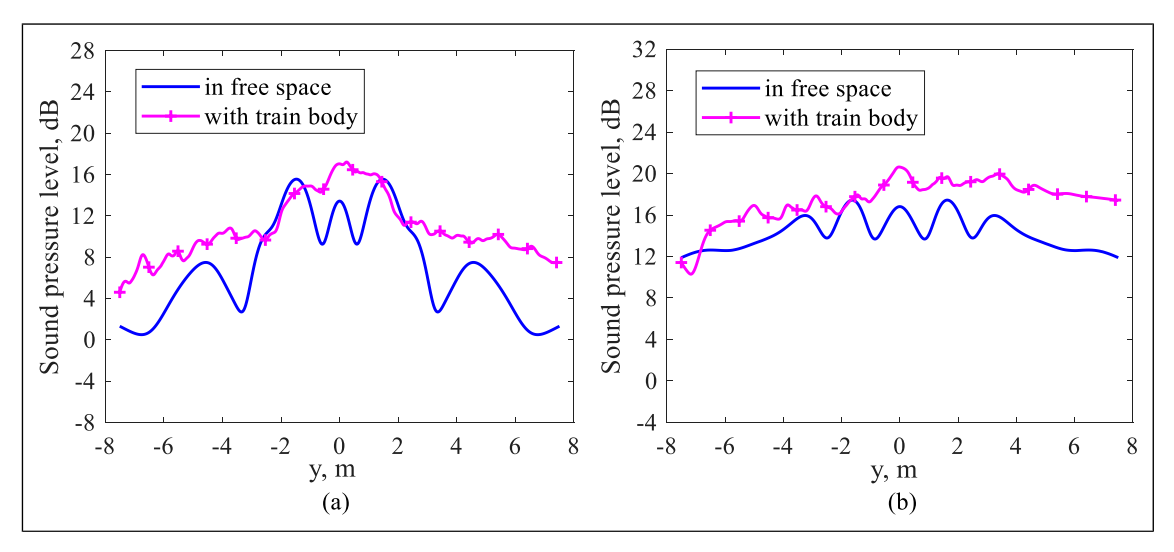


Figure 6. Comparison of the directivity under different conditions in terms of sound pressure level for a unit harmonic force averaged over frequency bands 50–5000 Hz. (a) Vertical force; (b) lateral force.



**Figure 7.** Distribution of sound pressure level along a horizontal line, results for a unit harmonic force, averaged over frequency bands 50–4000 Hz. (a) Vertical force; (b) lateral force.

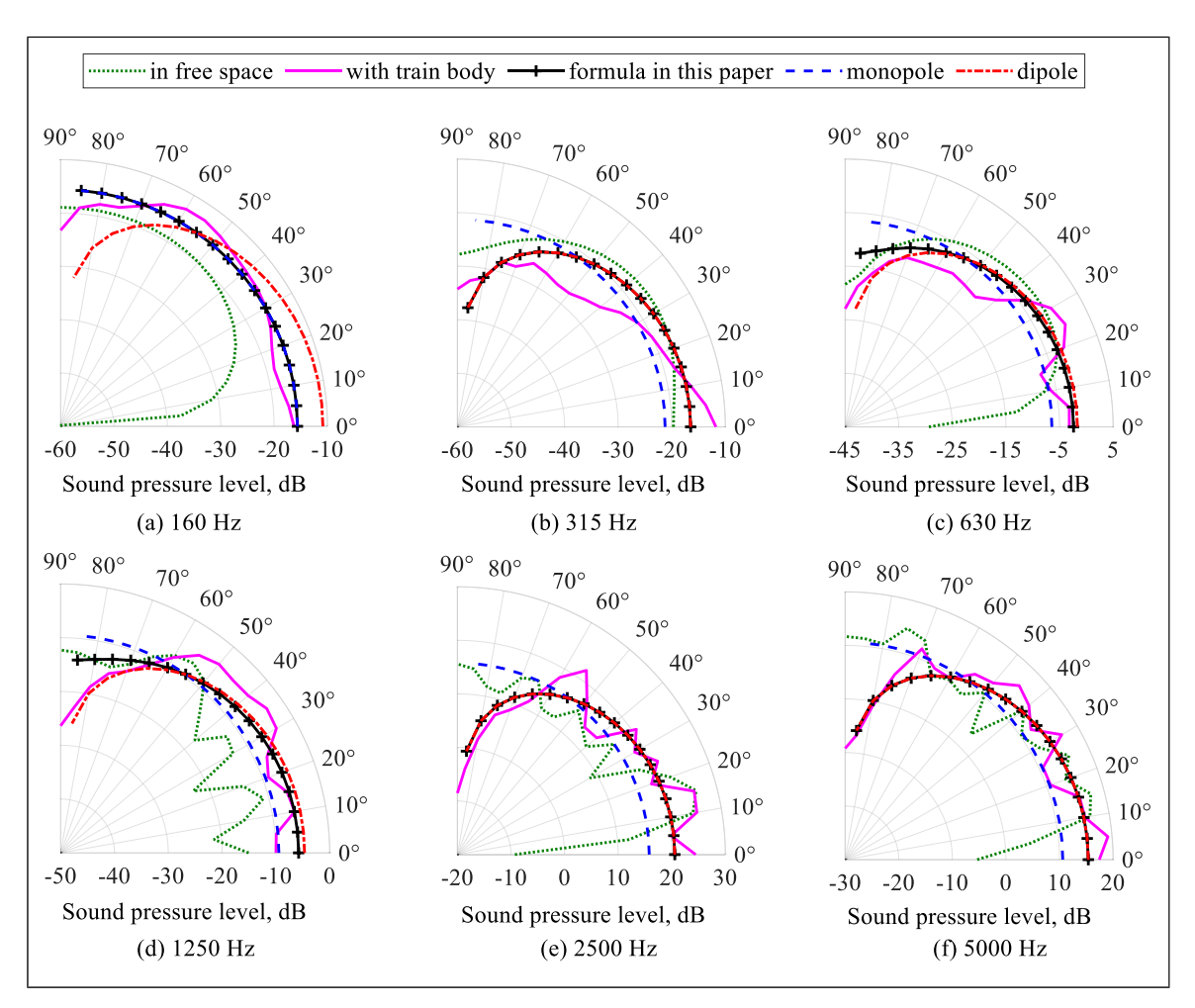


Figure 8. Comparison of wheel directivity in the vertical plane with monopole, dipole and a combination in one-third octave bands for a vertical unit force. (a) 160 Hz, (b) 315 Hz, (c) 630 Hz, (d) 1250 Hz, (e) 2500 Hz, (f) 5000 Hz.

Table 1 lists the values of a and b obtained for both the vertical and lateral excitation. As can be seen, for the vertical excitation at low frequencies (below 160 Hz), the wheel has the directivity of a monopole source, whereas it has the characteristics of dipole source at high frequencies (at and above 1600 Hz) where its

contribution is highest. In the middle frequency region, the predominance of monopole or dipole contributions varies between frequency bands. Similar trends are found for the lateral excitation of the wheel, although the directivity is closer to that of a dipole in most of the frequency range.

# Directivity in horizontal plane

For the directivity of the wheel in the direction along the track, a similar procedure was also followed as for the vertical plane. However, unlike for the vertical plane, the magnitude of the sound pressure curve was also added as a

variable in the regression analysis rather than fixing it according to equation (1). Results are shown in Figure 9 for vertical excitation. For this direction, the wheel again has the characteristics of a monopole at very low frequencies and a dipole at higher frequency, where additionally larger fluctuations of the directivity are present. For the lateral

Table 1. Coefficients for the wheel directivity in the presence of the train body.

Frequency, Hz	Vertical plane				Horizontal plane			
	Vertical excitation		Lateral excitation		Vertical excitation		Lateral excitation	
	а	ь	а	Ь	а	Ь	а	Ь
50	0.823	0.177	0.11	0.89	I	0	0.689	0.311
63	1	0	0.421	0.579	1	0	0.988	0.012
80	1	0	0.463	0.537	1	0	0.687	0.313
100	1	0	0.251	0.749	1	0	0	I
125	1	0	0.191	0.809	0	1	0.071	0.929
160	1	0	0.53	0.47	1	0	0.624	0.376
200	0.768	0.232	0.362	0.638	0	1	0.45	0.55
250	0.116	0.884	0.193	0.807	0	1	0.668	0.332
315	0	1	0.176	0.824	0	1	0	I
400	0.893	0.107	1	0	1	0	1	0
500	0.665	0.335	0.19	0.81	1	0	0.894	0.106
630	0.231	0.769	0.385	0.615	0	1	0	I
800	0.727	0.273	0	1	0	1	0	I
1000	0.36	0.64	0.261	0.739	0.58	0.42	0.397	0.603
1250	0.334	0.666	0	I	1	0	0.497	0.503
1600	0	1	0.432	0.568	0.44	0.56	1	0
2000	0	1	0	I	0	1	0	I
2500	0	1	0.002	0.998	0	1	0	I
3150	0	1	0	1	0	1	0	1
4000	0	1	0	I	0	I	0	I
5000	0	1	0	I				

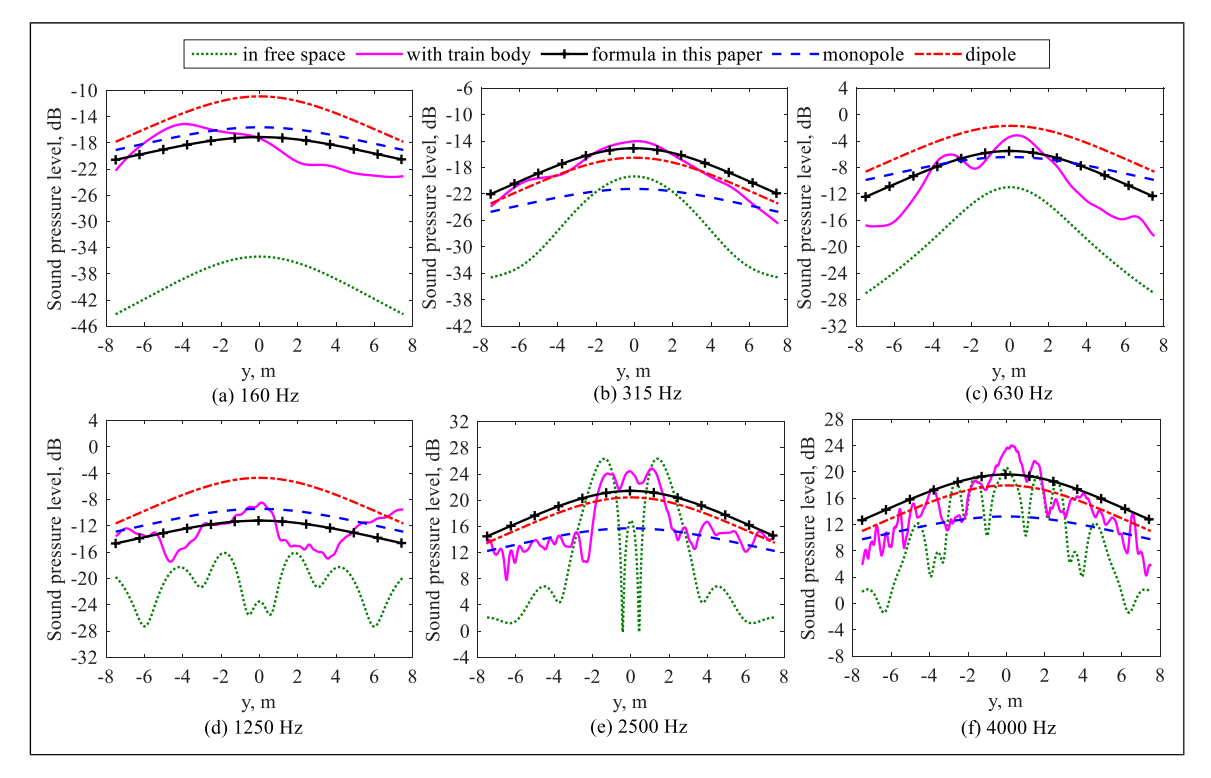


Figure 9. Distribution of sound pressure from the wheel parallel to the track in the presence of the train body for a vertical unit force.. (a) 160 Hz, (b) 315 Hz, (c) 630 Hz, (d) 1250 Hz, (e) 2500 Hz, (f) 4000 Hz.

excitation (not shown), the wheel more closely resembles a dipole in the whole frequency range. The corresponding values of a and b in these two cases are listed in Table 1. Figure 9 also shows the comparison with the sound radiation from the wheel in free space. The radiation pattern in the presence of the train body differs from that in free space, especially at low frequency, but they are closer to each other at high frequency. In some cases, the radiation pattern of the wheel in free space is even more directional than a dipole.

# **Conclusions**

The effect of the various structures in close proximity to a railway wheel on its sound radiation in situ is investigated by using a combination of FEM and the Boundary Element Method with Adaptive Order. The sound power, the sound pressure and the directivity are predicted for excitation by a unit force at the wheel/rail contact point in vertical and lateral directions. Results are compared for a wheel in free space, above a rigid ground, directly above the rail, in the presence of the bogic frame and installed under the train body.

It is found that the presence of these structures has little influence on the radiated sound power except at low frequency. The presence of the rail and the bogie frame has little effect on the vertical directivity of the wheel, whereas including the car body has a greater influence on the vertical directivity in the whole frequency range. Nevertheless, the effect is mainly to redistribute the lobes, whereas the overall trends are not greatly affected. The wheel directivity in the vertical plane has the characteristics of a monopole at low frequency and a dipole at higher frequency, irrespective of the excitation direction. Similarly, the horizontal directivity, in the direction along the track, has the properties of a monopole at very low frequencies and resembles a dipole at higher frequencies. The presence of the car body has only small effects of this wheel sound radiation pattern, but the sound pressure levels are increased to some extent. Empirical formulae for the wheel directivity including the influence of the train body are finally proposed, based on a combination of monopole and dipole contributions. These can be used in engineering models for rolling noise, e.g., Refs. 6–8, to determine the sound pressure during a train pass-by from the sound powers.

# Acknowledgements

The authors are grateful to Xubo Bai and to staff of Siemens Digital Industries Software for their technical assistance.

#### **Declaration of conflicting interests**

The author(s) declared no potential conflicts of interest with respect to the research, authorship, and/or publication of this article.

#### **Funding**

The author(s) disclosed receipt of the following financial support for the research, authorship, and/or publication of this article: The work described here has been supported by the National Natural Science Foundation of China (NSFC) under the grant 12104341 and the Royal Society under the grant IEC\NSFC\223195.

#### **ORCID iDs**

#### **Data Availability Statement**

Published data is available from the University of Southampton online repository at: https://doi.org/10.5258/SOTON/D3487<sup>24</sup>.

#### References

- Thompson D. Railway noise and vibration: mechanisms, modelling and means of control. 2nd ed. Elsevier Science, 2024.
- Remington PJ. Wheel/rail noise, Part IV: rolling noise. J Sound Vib. 1976; 46(3): 419–436.
- 3. Schneider E, Popp K and Irretier H. Noise generation in railway wheels due to rail-wheel contact forces. *J Sound Vib* 1988; 120: 227–244.
- Thompson DJ. Predictions of acoustic radiation from vibrating wheels and rails. J Sound Vib. 1988; 120: 275–280.
- Fingberg U. Ein Modell für das Kurvenquietschen von Schienenfahrzeugen. VDI Fortschritt-berichte, Reihe 11, Nr. 140, 1990.
- 6. Thompson DJ and Jones CJC. Sound radiation from a vibrating railway wheel. *J Sound Vib*. 2002; 253(2): 401–419.
- 7. Thompson DJ, Fodiman P and Mahé H. Experimental validation of the TWINS prediction program for rolling noise, part 2: results. *J Sound Vib.* 1996; 193(1): 137–147.
- 8. Thompson DJ, Hemsworth B and Vincent N. Experimental validation of the TWINS prediction program for rolling noise, part 1: description of the model and method. *J Sound Vib*. 1996; 193(1): 123–135.
- 9. Cheng G, He Y, Han J, et al. An investigation into the effects of modelling assumptions on sound power radiated from a high-speed train wheelset. *J Sound Vib* 2021; 495: 115910.
- Knuth C, Squicciarini G, Thompson D, et al. Effects of rotation on the rolling noise radiated by wheelsets in highspeed railways. *J Sound Vib* 2024; 572: 118180.
- 11. Thompson DJ. Wheel-rail noise generation, part V: inclusion of wheel rotation. *J Sound Vib.* 1993; 161(3): 467–482.
- 12. Sheng X, Peng Y and Xiao X. Boundary integral equations for sound radiation from a harmonically vibrating body moving uniformly in a free space. *J Acoust Soc Am* 2019; 146(6): 4493–4506.
- Sheng X, Cheng G and Thompson D. Modelling wheel/rail rolling noise for a high-speed train running along an infinitely long periodic slab track. *J Acoust Soc Am* 2020; 148(1): 174–190.
- 14. Theyssen J, Deppisch T, Pieringer A, et al. On the efficient simulation of pass-by noise signals from railway wheels. *J Sound Vib* 2023; 564: 117889.
- 15. Zhang X and Jonasson H. Directivity of railway noise sources. *J Sound Vib* 2006; 293(3): 995–1006.
- Fabre F, Theyssen J, Pieringer A, et al. Sound radiation from railway wheels including ground reflections: a half-space formulation for the Fourier boundary element method. *J Sound Vib* 2021; 493: 115822.

- 17. Heng C. Vertical directivity of train noise. *Appl Acoust* 1997; 51(2): 157–168.
- 18. Zhang X, Bai X, Thompson D, et al. Geometrical influence of structures in close proximity to a railway wheel on its sound radiation. The 52nd International Congress and Exposition on Noise Control Engineering, 2023.
- 19. Atak O, Li Y, Hamiche K, et al. *BEMAO*: a novel adaptive and high-order *BEM solver for steady-state acoustics-Part 1:* theory. Leuven: ISMA2022, 2022.
- 20. Hamiche K, Atak O, Li Y, et al. *BEMAO: a novel adaptive and high-order BEM solver for steady-state acoustics Part 2: application.* Leuven: ISMA2022, 2022.
- 21. Hamiche K, Li Y, Atak O, et al. A novel high-order and adaptive boundary element method solver (BEMAO) for small and large acoustics problems. Hamburg: DAGA2023, 2023.
- 22. Bai X, Zhang X and Li Y. Efficient calculating of the vibroacoustic behaviour of railway wheel based on Boundary Element Method with Adaptive Order. *J East China Jiaot Univ* 2024; 41(5): 48–55.
- 23. Fahy F and Thompson D. Fundamentals of sound and vibration. 2nd ed. Boca Raton FL: CRC Press, 2015.
- 24. Zhang X and Thompson D. The directivity of noise radiated by a railway wheel in situ. University of Southampton, 2025. DOI: 10.5258/SOTON/D3487.